Fibronectin Stimulates Endothelial Cell ^{18}F-FDG Uptake Through Focal Adhesion Kinase–Mediated Phosphatidylinositol 3-Kinase/Akt Signaling

Jin-Young Paik, Bong-Ho Ko, Kyung-Ho Jung, and Kyung-Han Lee

Department of Nuclear Medicine, Samsung Medical Center, Sungkyunkwan University School of Medicine, Seoul, Korea

There has been recent interest in the relationship between ^{18}F-FDG uptake and the angiogenic activity of endothelial cells (ECs). The angiogenic process is strongly dependent on the interaction of ECs with matrix fibronectin (FN), a key regulator of EC survival, migration, and proliferation. Therefore, we investigated how FN influences EC glucose uptake and elucidated the signaling pathways that mediate this effect. **Methods:** Human umbilical vein ECs were allowed to adhere to FN-coated plates and were compared with control cells for ^{18}F-FDG uptake, membrane GLUT1 levels, and hexokinase activity. The roles of focal adhesion kinase (FAK), phosphatidylinositol 3-kinase (PI3K), and Akt were evaluated with Western blotting, small interfering RNA (siRNA), and specific inhibitors. **Results:** FN adhesion significantly enhanced the protein-corrected ^{18}F-FDG uptake in HUVEC, to 2.1-, 2.7-, and 4.3-fold that in control cells by 2, 3, and 5 d, respectively. This effect was mediated by the upregulation of both membrane GLUT1 expression and hexokinase activity and was accompanied by FAK activation. Silencing of FAK signaling by siRNA completely abrogated both FN-induced FAK phosphorylation and ^{18}F-FDG uptake. FN also activated PI3K and Akt, well-known angiogenesis mediators, and the inhibition of either pathway totally abolished the effect of FN on ^{18}F-FDG uptake. Nitric oxide, a downstream Akt effector that stimulates glucose uptake, was not involved in the metabolic effect of FN. **Conclusion:** The results of this study demonstrated that an EC–FN interaction induces strong enhancement of ^{18}F-FDG uptake through the upregulation of GLUT1 expression and hexokinase activity. The findings also showed that the response occurs through FAK-mediated activation of PI3K and Akt, indicating a role for this pathway in modulating EC glucose metabolism.

Key Words: endothelial cell; fibronectin; ^{18}F-FDG, angiogenesis; focal adhesion kinase

J Nucl Med 2009; 50:618–624
DOI: 10.2967/jnumed.108.059386

Received Oct. 23, 2008; revision accepted Dec. 29, 2008.
For correspondence contact: Kyung-Han Lee, Department of Nuclear Medicine, Samsung Medical Center, 50 Ilwondong, Kangnamgu, Seoul, Korea.
E-mail: khleenm@yahoo.co.kr

Endothelial cells (ECs) have recently gained attention as an important nontumor cellular component of significant glucose use and ^{18}F-FDG uptake (*1–5*). ECs take up ^{18}F-FDG avidly in magnitudes comparable to or even greater than those of tumor cells and macrophages (*2*) and cause high levels of ^{18}F-FDG uptake in tumors of vascular endothelial origin (*6,7*). An issue of particular interest in EC ^{18}F-FDG uptake is its relationship to angiogenic activity, a fundamental step in tumor growth and ischemic injury healing. Observations in patients with cancer have shown tumors to have ^{18}F-FDG kinetics that are modulated by angiogenesis-related gene expression (*8*), and in some instances ^{18}F-FDG uptake has been correlated with histologic markers of angiogenesis (*9,10*). These findings likely reflect the increased metabolic activity of tumor cells but may also be partly attributable to the augmented ^{18}F-FDG uptake in activated endothelia in angiogenic vessels. Indeed, a positive influence on ^{18}F-FDG uptake was suggested in studies in which ECs were treated with angiogenic stimuli such as vascular endothelial growth factor (*2*), nitric oxide (NO) (*4*), and hypoxia (*5*).

Crucial for activation of the angiogenic process, however, are EC attachment to and interaction with the extracellular matrix (ECM); the latter, in turn, transmits signal cascades that mediate major angiogenic responses, including EC proliferation and migration (*11*). Because the performance of these functions requires increased energy expenditure (*4,12,13*) and EC energy is predominantly generated by glycolysis (*12,14*), it is plausible that an interaction with the ECM induces intracellular signals that augment glucose use and ^{18}F-FDG uptake.

Fibronectin (FN), a high-molecular-weight glycoprotein abundant in the matrix, is the foremost angiogenesis-associated ECM component promoting EC adhesion, proliferation, migration, and survival (*11,15–17*). The attachment of EC surface receptors to FN results in the transmission of intracellular signals through the activation of focal adhesion kinase (FAK), a nonreceptor tyrosine kinase that localizes to

regions of focal adhesion (*18,19*). Activated FAK, in turn, triggers several signaling pathways that regulate EC functions such as cell cycle progression, spreading, and survival. The autophosphorylation of FAK creates a binding site for the regulatory p85 subunit of phosphatidylinositol 3-kinase (PI3K), which can activate the catalytic p110 subunit and the PI3K/Akt signaling cascade (*20,21*). This pathway is a highly plausible candidate for mediating the enhancement of ^{18}F-FDG uptake in activated ECs because, although it is a well-recognized regulator of cell growth, survival, and angiogenesis, it also plays an important role in promoting glucose metabolism (*22–25*).

Elucidation of how an interaction with FN regulates EC glucose metabolism could provide insight into the contribution of angiogenic activity to ^{18}F-FDG uptake and how ECs are guaranteed a sufficient supply of energy to execute angiogenic processes. In this study, we investigated the influence of FN on EC ^{18}F-FDG uptake and explored the potential roles of FAK and downstream PI3K and Akt pathways in mediating this metabolic response.

MATERIALS AND METHODS

Cell Culture

Human umbilical vein ECs (HUVEC) were obtained from the American Type Culture Collection and maintained in EC basal medium (Clonetics) supplemented with epidermal growth factors, 12% fetal bovine serum, glucose at 2 g/L, and penicillin–streptomycin at 100 U/mL. Cells were cultured in a humidified atmosphere of 5% CO_2 at 37°C, the medium was changed every 3 d, and only cells from passages 4 and 5 were used.

For FN coating, the surface of standard polystyrene-treated culture plates (Corning Inc.) was covered with phosphate-buffered saline (PBS, pH 7.4) containing FN (10 μg/mL; Sigma Chemical Co.), and the plates were incubated at 37°C for 24 h. HUVEC were used to seed FN-coated or uncoated 12-well culture plates at 10^5 cells per well for experiments.

Evaluation of Cell Proliferation and ^{18}F-FDG Uptake

Cell morphology was inspected with hematoxylin–eosin staining, and cell proliferation was assessed by Bradford protein assays and 3-(4,5-dimethylthiazol-2-yl)-2,5-diphenyltetrazolium bromide (MTT) assays.

^{18}F-FDG uptake was measured 48 h after seeding, when cell confluence reached 80%. The use of culture medium rather than PBS enabled ^{18}F-FDG uptake to be measured at 37°C, thereby providing information more relevant to in vivo conditions than measuring uptake at 4°C. Thus, cells were incubated with 370 kBq (10 μCi) of ^{18}F-FDG added to the culture medium at 37°C for 40 min in 5% CO_2, rapidly washed twice with cold PBS, and lysed in 1 mL of distilled water. Cell-associated radioactivity was measured with a high-energy γ-counter (Wallac), and protein-corrected ^{18}F-FDG uptake levels expressed as a percentage of the level in control cells were calculated.

Measurements of Hexokinase Activity and NO Concentration

Total cellular hexokinase activity was measured by the method of Vinuela et al. as modified by Waki et al. (*26*). In brief, cells were homogenized in a buffer containing 50 mM triethanolamine and 5 mM $MgCl_2$ (pH 7.6), and a supernatant was obtained after centrifugation at 1,000*g* for 5 min at 4°C. The same type of buffer containing 0.5 mM glucose, 5 mM adenosine triphosphate, 0.25 mM reduced nicotinamide adenine dinucleotide phosphate, and 6 U of glucose 6-phosphate dehydrogenase was preincubated at 20°C for 15 min. Cell lysate samples were added, and the absorbance of the reaction mixture was measured. Hexokinase activity was determined from a standard curve, with 1 U being defined as enzyme activity that phosphorylated 1 μmol of glucose per minute at 20°C. Aliquots were removed to measure the protein content, and enzyme activity was expressed as a percentage of that in control cells.

For measurement of the concentration of NO released, 100 μL of medium was taken from culture plates 48 h after seeding. The medium was mixed with an equal volume of Griess reagent, which contained 1% sulfanilamide, 0.1% *N*-(1-naphthyl)ethylenediamine dihydrochloride, and 2.5% phosphoric acid. After incubation for 10 min, the absorbance at 540 nm was measured with a spectrophotometer, and the results were expressed as the NO concentration relative to that in control cells. The effect of exogenous NO was evaluated by adding 10–100 μM of sodium nitroprusside (SNP) (Sigma Chemical Co.) to the cell medium and incubating the mixture in a humidified atmosphere of 5% CO_2 at 37°C for 24 h.

Western Blotting of Membrane GLUT1

For the analysis of membrane GLUT1 expression, two 150-mm plates of 80% confluent HUVEC were washed twice with PBS. The cells were solubilized with 500 μL of a lysis buffer containing sucrose (0.0856 g/mL), *N*-2-hydroxyethylpiperazine-*N*′-2-ethanesulfonic acid (HEPES) (10 mmol/mL), ethylenediaminetetraacetic acid (EDTA) (25 μmol/mL), aprotinin (10 μg/mL), leupeptin (10 μg/mL), and phenylmethylsulfonyl fluoride (1 mM). After centrifugation at 1,000*g* for 20 min, the supernatant was collected and incubated with 1.5 mL of a lysis buffer containing sucrose (0.0856 g/mL), HEPES (10 mmol/mL), and $MgCl_2$ (10 mmol/mL) at 4°C for 1 h. The mixture was centrifuged at 45,000 rpm for 60 min, and the pellet was dissolved in a minimum volume of PBS. Membrane proteins were separated on a 10% polyacrylamide gel, electroblotted to a Hybond enhanced chemiluminescence nitrocellulose membrane (Amersham), and reacted with a polyclonal antibody against human GLUT1 (1:1,000 dilution; Calbiochem). GLUT1 protein was visualized by incubation with a horseradish peroxidase–conjugated secondary antirabbit IgG antibody (1:1,000 dilution; Caltag), 1 min of soaking in Amersham ECL Western Blotting Detection Reagent (GE Healthcare), and detection of signals on a high-performance chemiluminescence film. Protein band intensities on the film were measured with a GS-800 calibrated densitometer and Quantity One software (both from Bio-Rad Laboratories).

Western Blotting of Phosphorylated FAK (p-FAK), Phosphorylated PI3K (p-PI3K), and Phosphorylated Akt (p-Akt)

For the analysis of p-FAK protein, cells from 100-mm culture plates were washed, lysed, and sonicated for 10–15 s to reduce sample viscosity. After the lysate was heated to 95°C for 5 min and centrifuged at 15,000*g* for 5 min, the proteins were separated on a 10% polyacrylamide gel, electroblotted, and visualized as described earlier after reaction with a polyclonal antibody against human p-FAK (pY397; BD Biosciences) at a 1:1,000 dilution and a horseradish peroxidase–conjugated secondary sheep antimouse

IgG antibody (GE Healthcare) at a 1:1,000 dilution. For p-FAK and GLUT1 immunoblots, 20-μg samples were loaded in each lane after protein assays, and the similarity of protein loading among lanes was confirmed by Ponceau S staining of the membranes without the use of a loading control protein.

For the analysis of p-PI3K and p-Akt proteins, cells from 100-mm culture plates (after 24 h of adhesion) were washed and solubilized at room temperature with 1 mL of a radioimmunoprecipitation buffer containing Tris base (0.079 g/mL), NaCl (0.09 g/mL), NP-40 (10%; Sigma-Aldrich), EDTA (10 μmol/L), aprotinin (10 μg/mL), leupeptin (10 μg/mL), and phenylmethylsulfonyl fluoride (1 mM). After centrifugation at 14,000*g* for 15 min, supernatants were incubated with 100 μL of precleared protein A–Sepharose beads (Sigma-Aldrich) at 4°C for 10 min to reduce nonspecific binding. The beads were then removed by centrifugation, and total cell protein was diluted to 1 mg/mL with PBS to reduce the concentrations of detergents. The collected protein was mixed with an antibody against p-PI3K (500:1; Santa Cruz Biotechnology) or p-Akt (200:1; Cell Signaling Technology), and the mixture was incubated at 4°C for 2 h on a shaker. The immunocomplex was captured by adding 50 μL of a protein A–Sepharose bead slurry and gently rocking the mixture on a shaker overnight at 4°C. The immunoprecipitate was collected by centrifugation and 2–4 washes of the pellet with 1.0 mL of the radioimmunoprecipitation buffer. After the final wash, the pellet was suspended in 50 μL of 2× electrophoresis sample buffer, and the mixture was boiled for 4 min. The proteins were separated on a 10% polyacrylamide gel, electroblotted, and incubated with the same polyclonal antibody against human p-PI3K (1:500 dilution) or human p-Akt (1:200 dilution) as that used for immunoprecipitation. p-PI3K and p-Akt bands were visualized with horseradish peroxidase–conjugated secondary antigoat and antirabbit IgG antibodies (both at a 1:1,000 dilution; Santa Cruz Biotechnology), respectively.

Silencing of FAK Signaling by Small Interfering RNA (siRNA) Transfection

For the silencing of FAK signaling, cells were transfected with target-specific 20- to 25-nucleotide siRNA designed to decrease FAK gene expression in human cells (SC-29310; Santa Cruz Biotechnology). Transfection was accomplished with a Signal-Silence kit (Cell Signaling Technology) according to the recommended protocol. In brief, 2 μL of transfection reagent was added to 100 μL of serum-free medium in a sterile tube, and the mixture was incubated at room temperature for 5 min. FAK-inactivating siRNA was added to a final concentration of 100 nM, and the mixture was incubated for another 5 min. This final mixture was added to the culture medium of 60% confluent cells that had been used to seed 12-well plates 24 h earlier. After vigorous agitation to allow the even dispersion of siRNA, cells were incubated in a humidified atmosphere of 5% CO_2 at 37°C. The medium was replaced with fresh medium 3 d later, and ^{18}F-FDG uptake was measured the next day.

Inhibition of Kinases and NO Synthase

Candidate signaling pathways were evaluated by adding specific kinase inhibitors to the medium 48 h before ^{18}F-FDG uptake experiments. PI3K was blocked by 10 μM LY294002 or 200 nM wortmannin, and Akt was blocked by a 1 μM concentration of a cell-permeating benzimidazole compound (Akt inhibitor IV; molecular formula, $C_{31}H_{27}IN_4S$; Calbiochem) that inhibits Akt phosphorylation without affecting PI3K activity.

Blocking of NO release was achieved by adding N^G-nitro-L-arginine methyl ester (L-NAME; RBI) at a concentration of 0.05–1 mM to the medium 48 h before ^{18}F-FDG uptake measurements.

Statistical Analysis

All ^{18}F-FDG uptake data and hexokinase assay data are the summed results of 2 or 3 independent experiments performed in triplicate. All values shown represent the mean ± SD. Student's test was used to evaluate statistical significance between groups, and P values of <0.05 were considered significant.

RESULTS

FN Interaction Augments HUVEC ^{18}F-FDG Uptake

Microscopic inspection revealed little alteration in HUVEC morphology by FN. MTT and protein assays revealed a proliferative effect after 3 d of FN treatment (protein contents were 149.0% ± 8.1% and 249.0% ± 3.2% those in control cells at days 3 and 5, respectively). FN significantly enhanced ^{18}F-FDG uptake in a manner that preceded and surpassed its proliferative effect. Hence, even after correction for protein content, the ^{18}F-FDG uptake in FN-treated cells was increased to 210%, 268%, and 431% that in control cells at 2, 3, and 5 d, respectively. On the basis of these findings, the remaining ^{18}F-FDG uptake experiments were performed 48 h after seeding to exclude effects from cell proliferation.

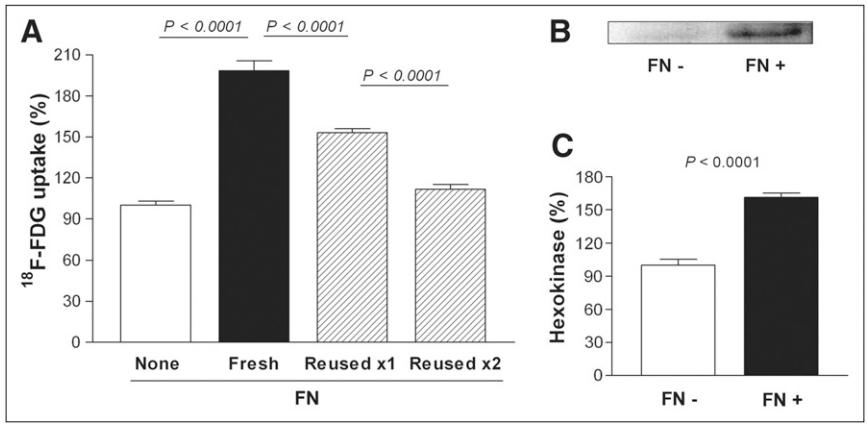

FIGURE 1. Effects of FN on ^{18}F-FDG uptake, GLUT1 expression, and hexokinase activity. (A) ^{18}F-FDG uptake in HUVEC treated with fresh or reused FN relative to that in nontreated control cells. Data are mean ± SD of 3 independent experiments. (B) Representative Western blot of plasma membrane GLUT1 protein in FN-treated (FN+) and non–FN-treated (FN−) cells. (C) Total cellular hexokinase activity relative to that in control cells. Data are mean ± SD of 2 independent experiments.

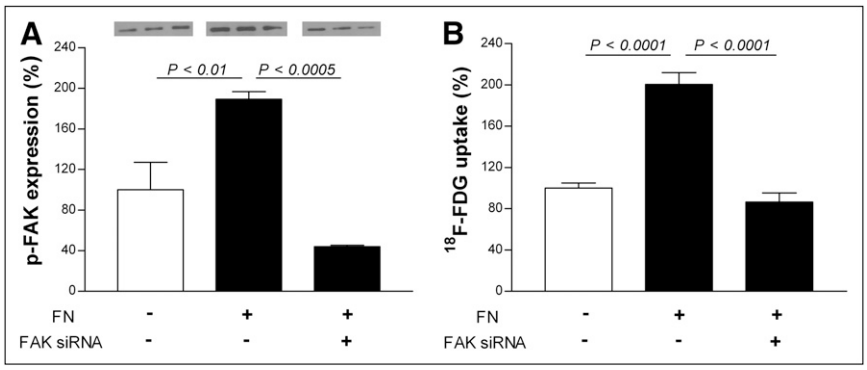

FIGURE 2. Effect of FAK silencing by siRNA transfection on p-FAK levels (A) and ^{18}F-FDG uptake (B). ^{18}F-FDG uptake data are mean ± SD of 2 independent experiments.

The specificity of the effect of FN was evaluated by using FN with graded degrees of degradation through repeated use. With fresh FN, there was a significant increase in ^{18}F-FDG uptake, which reached 198.6% ± 7.2% that in control cells (Fig. 1A). However, FN reused once and twice had proportionally attenuated stimulatory effects on ^{18}F-FDG uptake—153.2% ± 6.6% and 111.7% ± 8.3% that of control cells, respectively—indicating that the effect was specific for intact FN protein (Fig. 1A).

FN Enhances Membrane GLUT1 Expression and Hexokinase Activity

Western blotting of HUVEC treated with FN for 2 d revealed an increase in the expression of membrane GLUT1 protein, the main glucose transporter in ECs, compared with that in control cells (Fig. 1B). Furthermore, FN treatment for 2 d induced a significantly higher level of total cellular hexokinase activity, which reached 1.6 ± 0.0-fold that in control cells (Fig. 1C).

FAK Silencing Completely Abrogates FN-Stimulated ^{18}F-FDG Uptake

p-FAK protein band densities were significantly increased by FN treatment, to 189.2% ± 7.2% that in control cells (Fig. 2A). However, silencing of FAK signaling by siRNA transfection completely blocked this effect, with p-FAK protein being reduced to a level lower than that in control cells (44.0% ± 2.6%) (Fig. 2A). Blocking of FAK signaling by siRNA also completely abolished FN-stimulated ^{18}F-FDG uptake, from 200.7% ± 11.4% to 86.6% ± 19.4% that in control cells (Fig. 2B).

FN-Stimulated ^{18}F-FDG Uptake Is Mediated Through PI3K/Akt Pathway

FN significantly increased HUVEC p-PI3K (Fig. 3A) and p-Akt (Fig. 3B) protein levels. Furthermore, FN-stimulated ^{18}F-FDG uptake was effectively blocked by the specific PI3K inhibitors wortmannin and LY294002 and by Akt inhibitor IV to 58.5% ± 12.1%, 52.0% ± 7.9%, and 53.0% ± 1.8% uninhibited levels, respectively (Figs. 4A and 4B). These results indicated that FN-stimulated ^{18}F-FDG uptake occurs through the PI3K/Akt pathway.

NO Signaling Is Not Involved in FN-Stimulated ^{18}F-FDG Uptake

The possible involvement of NO was evaluated because it is a major downstream effector of Akt signaling and is capable of stimulating EC ^{18}F-FDG uptake. Exogenous donation of NO by the addition of 10 and 100 μM SNP indeed increased ^{18}F-FDG uptake in non–FN-treated cells to 213.3% ± 9.0% and 238.3% ± 8.3% that in nonstimulated control cells, respectively, and in FN-treated cells from 225.7% ± 38.0% to 230.4% ± 33.7% and 254.% ± 17.4% that in nonstimulated control cells, respectively (Fig. 5A). However, NO release was not increased by FN treatment, regardless of whether or not SNP was added (Fig. 5B). Furthermore, blocking of NO synthase with various doses of L-NAME had no effect on FN-stimulated ^{18}F-FDG uptake (Fig. 5C).

DISCUSSION

ECs are the primary effector cells for new vessel formation, a process critical for tumor growth and ischemic injury

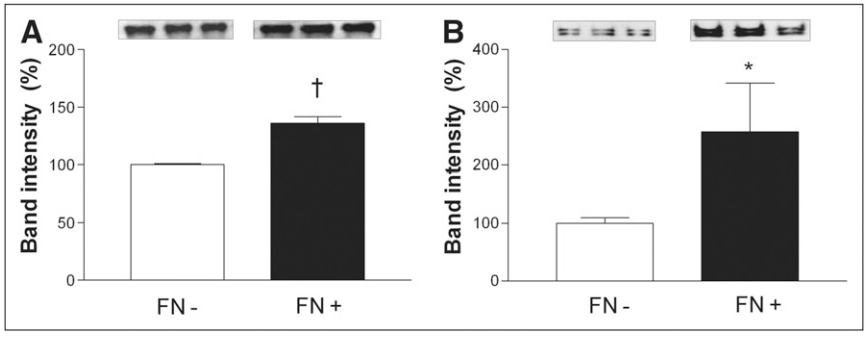

FIGURE 3. Western blot and band intensity of p-PI3K (A) and p-Akt (B) in FN-treated (FN+) and non–FN-treated (FN−) cells. Data are mean ± SD of band densities relative to that in control cells in triplicate samples. *$P < 0.05$ compared with control cell values. †$P < 0.001$ compared with control cell values.

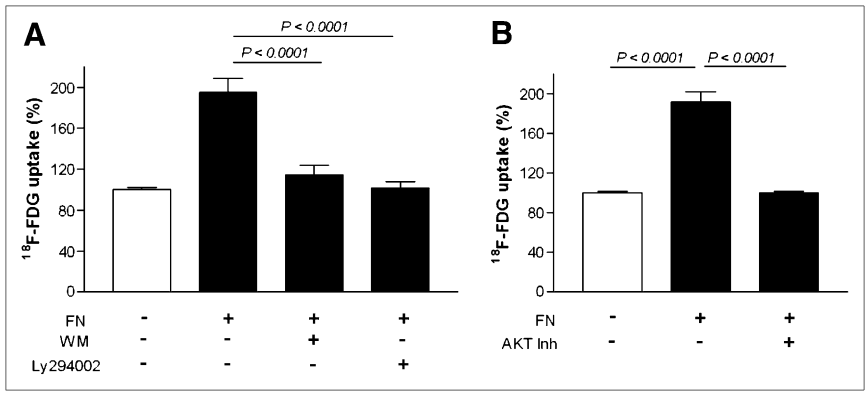

FIGURE 4. Effects of specific PI3K inhibitors (A) and Akt inhibitor (B) on FN-stimulated ^{18}F-FDG uptake. Data are mean ± SD of 3 independent experiments. AKT Inh, 1 μM Akt inhibitor IV; Ly294002, 10 μM LY294002; WM, 200 nM wortmannin.

healing. The execution of angiogenic responses requires an increase in energy supply, which in ECs is predominantly met with adenosine triphosphate generated from glycolysis (*13,14*). Thus, the molecular mechanisms that regulate EC glucose metabolism are of significant interest, particularly in relation to the influence of major angiogenic stimuli.

In the present study, we investigated the effect of an interaction with FN, a highly specialized glycoprotein that mediates a variety of ECM–cell interactions and that plays a pivotal role in angiogenesis (*11,15,16*), on HUVEC ^{18}F-FDG uptake. We found that FN stimulates significant enhancement of ^{18}F-FDG uptake and that this effect is mediated by the upregulation of both the expression of membrane GLUT1, the predominant EC glucose transporter (*27*), and the activity of hexokinase, the rate-limiting enzyme in glycolysis. Further exploration of the molecular mechanisms revealed the involvement of FAK and downstream PI3K/Akt signaling in the FN-induced metabolic effect.

We also found that attachment to FN led to an increase in the number of HUVEC compared with the number of control cells after 3 d. A similar proliferative effect of FN on ECs was previously observed (*28,29*). However, our findings demonstrated that FN-stimulated ^{18}F-FDG uptake clearly precedes and surpasses the increase in cell numbers, suggesting that the metabolic effect of FN is distinct from its proliferative effect.

To identify the signaling mechanism that mediated this metabolic effect, we explored the involvement of FAK, a cytoplasmic kinase that resides at focal adhesion sites and that links ECM-derived signals to the cell interior (*18,19*). Significant activation of FAK was observed in FN-treated HUVEC, and perturbation of FAK signaling by RNA interference completely abolished the augmentation of cellular ^{18}F-FDG uptake as well as FAK phosphorylation. FAK is a well-recognized mediator of growth factor signaling, cell proliferation, and migration in cancer cells (*18*) and has been implicated in EC functions that promote angiogenesis (*19*). Our findings indicated that FAK is involved in modulating EC glucose metabolism as well. A similar effect of FAK levels in regulating glucose uptake in C2C12 skeletal muscle cells was recently observed by Bisht et al. (*30*).

In the study of Bisht et al., the effect of FAK on skeletal myocyte glucose metabolism appeared to be mediated mainly through PI3K and protein kinase C rather than Akt (*30*). In the present study, however, the FN-induced phosphorylation of FAK in HUVEC was accompanied by the activation of both PI3K and Akt. Furthermore, the inhibition of PI3K by wortmannin or LY294002 and the blocking

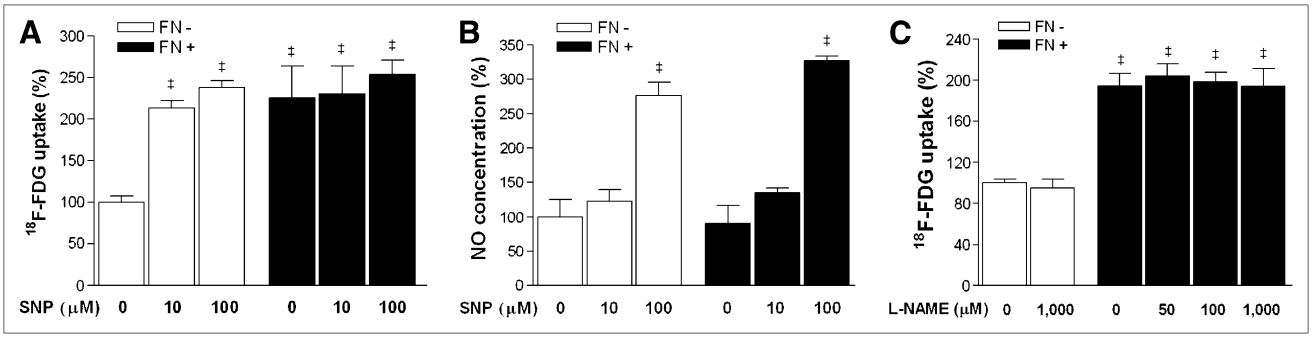

FIGURE 5. Role of NO in FN-stimulated ^{18}F-FDG uptake. (A) Effect of 10 and 100 μM SNP on ^{18}F-FDG uptake in FN-treated (FN+) and non–FN-treated (FN−) cells. (B) Concentration of released NO in culture medium with or without addition of SNP. (C) Effect of inhibition of NO synthase by L-NAME on ^{18}F-FDG uptake. ^{18}F-FDG uptake data are mean ± SD of 2 independent experiments. ‡$P < 0.0001$ compared with control cell values.

of Akt activity by a specific inhibitor completely abrogated the stimulatory effect of FN on ^{18}F-FDG uptake. Given the known instability of wortmannin in culture medium (*31*), it is possible that the actual inhibitory effect of this agent was even greater than that observed. In ECs, the PI3K/Akt signaling axis is activated by many angiogenic growth factors and critically regulates cell survival and angiogenesis (*22–25*). The PI3K/Akt pathway is also a well-recognized regulator of cellular glucose uptake and metabolism. The serine/threonine kinase Akt is activated in response to insulin and growth factors in a PI3K-dependent fashion and stimulates glucose uptake through the upregulation of glucose transporters and increased hexokinase activity (*25*). Our results implied a mechanism in ECs that is induced by FN-activated FAK signaling, similar to that induced by growth factor receptor activation in tumor cells, through which glucose uptake is promoted via activation of the PI3K/Akt pathway.

Because neovascularization plays a key role in the ability of malignant cells to grow and metastasize, many studies have focused on evaluating novel agents that inhibit angiogenesis as a method for controlling tumor growth. Elucidating the relationship among FN, EC glucose metabolism, and the FAK/PI3K/Akt signaling pathway may provide valuable insights into prospective targets for angiogenesis inhibition and mechanisms for assessing the efficacy of new potential therapeutic agents. A difficulty in the use of cultured EC models, however, is that the behaviors of cells derived from different organs or species as well as of cells originating from microvascular and large vessels can differ. Indeed, ECs from different origins have been described to vary with regard to glucose metabolism and transporter-related responses (*14*). Therefore, the results that we observed in the present study are limited to HUVEC.

We also evaluated whether NO signaling was involved in the FN-induced metabolic effect because Akt is known to stimulate NO release through NO synthase activation in ECs (*32*) and we had previously found NO to be a powerful simulator of ^{18}F-FDG uptake in ECs (*4*). However, our results showed that although NO could indeed stimulate ^{18}F-FDG uptake, FN-stimulated ^{18}F-FDG uptake was neither accompanied by elevated NO release nor attenuated by the inhibition of NO synthase, indicating that the metabolic effect of FN was independent of NO signaling.

CONCLUSION

The results of the present study demonstrated that FN enhances EC glucose uptake through the upregulation of membrane GLUT1 expression and hexokinase activity. Furthermore, the FN-induced metabolic response is mediated by FAK and downstream PI3K/Akt activation, indicating a role for this pathway in modulating EC glucose metabolism.

ACKNOWLEDGMENTS

This work was supported by a Korean Science and Engineering Foundation (KOSEF) grant funded by the Korea Government (M20702010003-08N0201-00312). This work was presented in part at the Joint Molecular Imaging Conference, September 8–11, 2007, Providence, RI.

REFERENCES

1. Xu W, Koeck T, Lara AR, et al. Alterations of cellular bioenergetics in pulmonary artery endothelial cells. *Proc Natl Acad Sci USA.* 2007;104:1342–1347.
2. Maschauer S, Prante O, Hoffmann M, Deichen JT, Kuwert T. Characterization of ^{18}F-FDG uptake in human endothelial cells in vitro. *J Nucl Med.* 2004;45:455–460.
3. Buck AK, Reske SN. Cellular origin and molecular mechanisms of ^{18}F-FDG uptake: is there a contribution of the endothelium? *J Nucl Med.* 2004;45:461–463.
4. Paik JY, Lee KH, Ko BH, Choe YS, Choi Y, Kim BT. Nitric oxide stimulates ^{18}F-FDG uptake in human endothelial cells through increased hexokinase activity and GLUT1 expression. *J Nucl Med.* 2005;46:365–370.
5. Oswald J, Treite F, Haase C, et al. Experimental hypoxia is a potent stimulus for radiotracer uptake in vitro: comparison of different tumor cells and primary endothelial cells. *Cancer Lett.* 2007;254:102–110.
6. Ergün EL, Lim E. Increased FDG uptake in pulmonary epithelioid hemangioendothelioma. *Rev Esp Med Nucl.* 2006;25:188–192.
7. Rest CC, Botton E, Robinet G, Conan-Charlet V, Bizais Y, Visvikis D. FDG PET in epithelioid hemangioendothelioma. *Clin Nucl Med.* 2004;29:789–792.
8. Strauss LG, Koczan D, Klippel S, et al. Impact of angiogenesis-related gene expression on the tracer kinetics of ^{18}F-FDG in colorectal tumors. *J Nucl Med.* 2008;49:1238–1244.
9. Cher LM, Murone C, Lawrentschuk N, et al. Correlation of hypoxic cell fraction and angiogenesis with glucose metabolic rate in gliomas using ^{18}F-fluoromisonidazole, ^{18}F-FDG PET, and immunohistochemical studies. *J Nucl Med.* 2006;47:410–418.
10. Guo J, Higashi K, Ueda Y, et al. Microvessel density: correlation with ^{18}F-FDG uptake and prognostic impact in lung adenocarcinomas. *J Nucl Med.* 2006;47:419–425.
11. Davis GE, Senger DR. Endothelial extracellular matrix: biosynthesis, remodeling, and functions during vascular morphogenesis and neovessel stabilization. *Circ Res.* 2005;97:1093–1107.
12. Mallery SR, Lantry LE, Laufman HB, Stephens RE, Brierley GP. Modulation of human microvascular endothelial cell bioenergetic status and glutathione levels during proliferative and differentiated growth. *J Cell Biochem.* 1993;53:360–372.
13. Culic O, Decking UKM, Schrader J. Metabolic adaptation of endothelial cells to substrate deprivation. *Am J Physiol Cell Physiol.* 1999;276:C1061–C1068.
14. Mann GE, Yudilevich DL, Sobrevia L. Regulation of amino acid and glucose transporters in endothelial and smooth muscle cells. *Physiol Rev.* 2003;83:183–252.
15. Dannen EH, Yamada KM. Fibronectin, integrins, and growth control. *J Cell Physiol.* 2001;189:1–13.
16. Kim S, Bell K, Mousa SA, Varner JA. Regulation of angiogenesis in vivo by ligation of integrin $\alpha5\beta1$ with the central cell-binding domain of fibronectin. *Am J Pathol.* 2000;156:1345–1362.
17. Berndorff D, Borkowski S, Moosmayer D, et al. Imaging of tumor angiogenesis using ^{99m}Tc-labeled human recombinant anti-ED-B fibronectin antibody fragments. *J Nucl Med.* 2006;47:1707–1716.
18. McLean GW, Carragher NO, Avizienyte E, Evans J, Brunton VG, Frame MC. The role of focal-adhesion kinase in cancer: a new therapeutic opportunity. *Nat Rev Cancer.* 2005;5:505–515.
19. Peng X, Ueda H, Zhou H, et al. Overexpression of focal adhesion kinase in vascular endothelial cells promotes angiogenesis in transgenic mice. *Cardiovasc Res.* 2004;64:421–430.
20. Chen HC, Appeddu PA, Isoda H, Guan J-L. Phosphorylation of tyrosine 397 in focal adhesion kinase is required for binding phosphatidylinositol 3K. *J Biol Chem.* 1996;271:26329–26334.
21. Xia H, Nho RS, Kahm J, Kleidon J, Henke CA. Focal adhesion kinase is upstream of phosphatidylinositol 3-kinase/Akt in regulating fibroblast survival in response to contraction of type I collagen matrices via a beta 1 integrin viability signaling pathway. *J Biol Chem.* 2004;279:33024–33034.
22. Castellino RC, Durden DL. Mechanisms of disease: the PI3K-Akt-PTEN signaling node—an intercept point for the control of angiogenesis in brain tumors. *Nat Clin Pract Neurol.* 2007;3:682–693.
23. Shiojima I, Warsh K. Role of Akt signaling in vascular homeostasis and angiogenesis. *Circ Res.* 2002;90:1243–1250.

24. Somanath PR, Razorenova OV, Chen J, Byzova TV. Akt1 in endothelial cell and angiogenesis. *Cell Cycle.* 2006;5:512–518.
25. Manning BD, Cantley LC. AKT/PKB signaling: navigating downstream. *Cell.* 2007;129:1261–1274.
26. Waki A, Kato H, Yano R, et al. The importance of glucose transport activity as the rate-limiting step of 2-deoxyglucose uptake in tumor cells in vitro. *Nucl Med Biol.* 1998;25:593–597.
27. Knott RM, Robertson M, Muckersie E, Forrester JV. Regulation of glucose transporters (GLUT-1 and GLUT-3) in human retinal endothelial cells. *Biochem J.* 1996;318:313–317.
28. Wang J, Milner R. Fibronectin promotes brain capillary endothelial cell survival and proliferation through alpha5beta1 and alphavbeta3 integrins via MAP kinase signalling. *J Neurochem.* 2006;96:148–159.
29. Wilson SH, Ljubimov AV, Morla AO, et al. Fibronectin fragments promote human retinal endothelial cell adhesion and proliferation and ERK activation through alpha5beta1 integrin and PI 3-kinase. *Invest Ophthalmol Vis Sci.* 2003;44:1704–1715.
30. Bisht B, Goel HL, Dey CS. Focal adhesion kinase regulates insulin resistance in skeletal muscle. *Diabetologia.* 2007;50:1058–1069.
31. Holleran JL, Egorin MJ, Zuhowski EG, Parise RA, Musser SM, Pan SS. Use of high-performance liquid chromatography to characterize the rapid decomposition of wortmannin in tissue culture media. *Anal Biochem.* 2003;323:19–25.
32. Dimmeler S, Flemming I, Fisslthaler B, Harmann C, Busse R, Zeiher AM. Activation of nitric oxide synthase in endothelial cells by Akt-dependent phosphorylation. *Nature.* 1999;399:601–605.